Electronic Supplementary Material (ESI) for Materials Advances.

Supporting Information

One-pot strategic construction of the functionalized nanomaterial ZIF-90-Rhn for stepwise detecting and capturing toward Ag^+, formaldehyde in aqueous solution

Xiaoyu Du[a]; Mengwen Li[a]; Man Du[b*]; Ao Shen[a]; Xiaohui Hao[a]; Jiaxin Yuan[a]; Shufeng Ma[a]; Yongwei Zhao[a]; Lala Hou[a]; Ziqi Li[a]; Yunxu Yang[a*]

[a] *Department of Chemistry and Chemical Engineering, School of Chemistry and Biological Engineering, University of Science and Technology Beijing, Beijing 100083, China.*

[b] *School of Chemical and Pharmaceutical Engineering, Hebei University of Science and Technology, Shijiazhuang, 050018, China.*

Corresponding Author: Yang Yunxu[a]; Du man[b].

E-mail addresses:

yxyang@ustb.edu.cn (Yang yunxu);

mandu@hebust.edu.cn (Du man);

Contents:

Materials and instrumentations

Imidazole-2-carboxaldehyde and propan-2-ol was purchased from J&K; Rhodanine-3-acetic acid was purchased from Shanghai Titan Scientific Co., Ltd; Polyvinylpyrrolidone was purchased from Shanghai Macklin Biochemical Co., Ltd; Silver nitrate was purchased from Aladdin. Zinc nitrate hexahydrate was purchased from Sino pharm Chemical Reagent Co., Ltd; silver standard solution was purchased Steel Yanak Co., LTD; Cy-N was homemade in the lab. All the other chemicals obtained from commercial sources were analytical pure and used without further purification. The water was purified by Millipore filtration system.

X-Ray Diffracter data (XRD) were obtained with Ultima IV multipurpose X-ray diffraction system (Japan). Fluorescence emission studies were carried out with a Hitachi F-4500 Flourescence Spectrophotometer. Fourier transform infrared (FT-IR) spectra were recorded in the region of 440-4000 cm^{-1} with a FTIR-8400s Fourier Transform Infrared Spectrometer (Shimadzu). The scanning electron microscope (SEM) was used Ultra-high Resolution Scanning Electron Microscope SU8010.Thermogravimetric Analysis data (TG) were obtained by a METTLER TOLEDO TGA/DSC1 Synchronous Thermal Analyzer. XPS studies were performed on a Physical Electronics spectrometer (PHI Versa Probe II Scanning XPS Microprobe) with scanning monochromatic X-ray Al Kα radiation (100 μm, 100 W, 20 kV, 1,486.6 eV) as the excitation source and with a dual-beam charge neutralizer. The Brunauer–Emmette–Teller (BET) surface area and pore size measurements of the prepared samples were recorded by N_2 adsorption/desorption analysis using an ASAP 2020 Micromeritics (USA). ^{1}H NMR spectra were measured on a Varian Gemin-400 MHz spectrometer with chemical shifts reported in ppm (TMS as internal standard). Ultraviolet visible (UV) absorption spectra were obtained by a UV-2600 spectrometer (Techcomp., China).

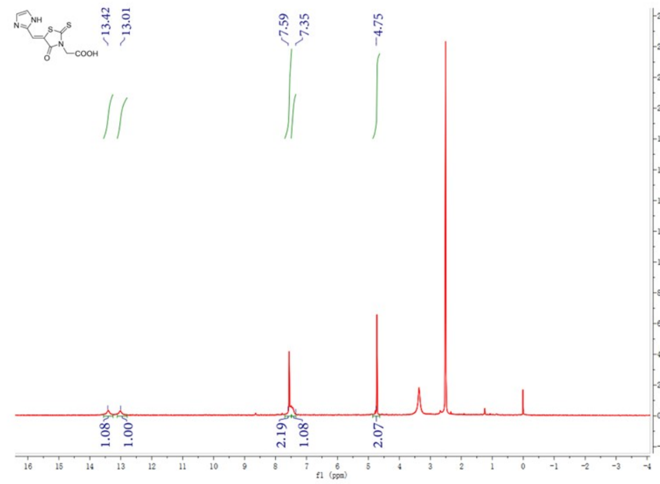

Fig. S1 ^{1}H NMR spectrum of **ligand 1**

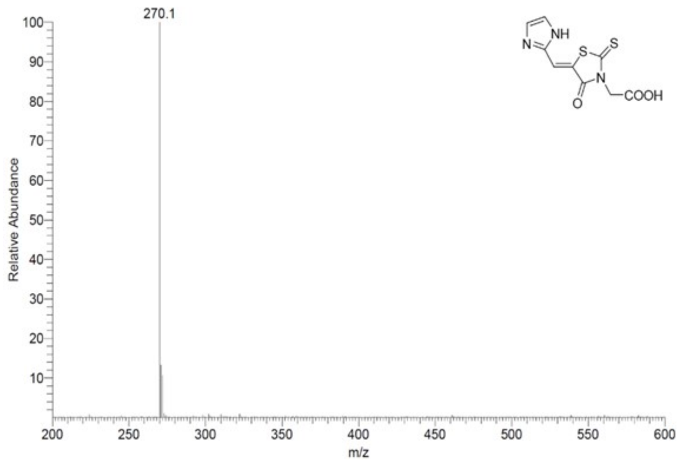

Fig. S2 ESI mass spectra spectrum of **ligand 1**

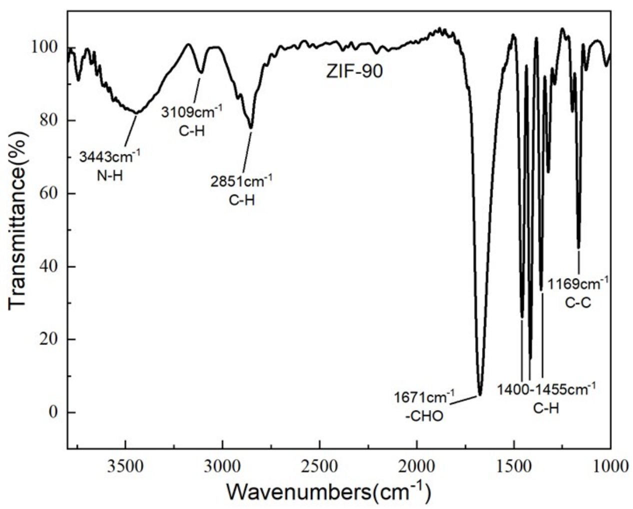

Fig. S3 The FT-IR spectra of ZIF-90

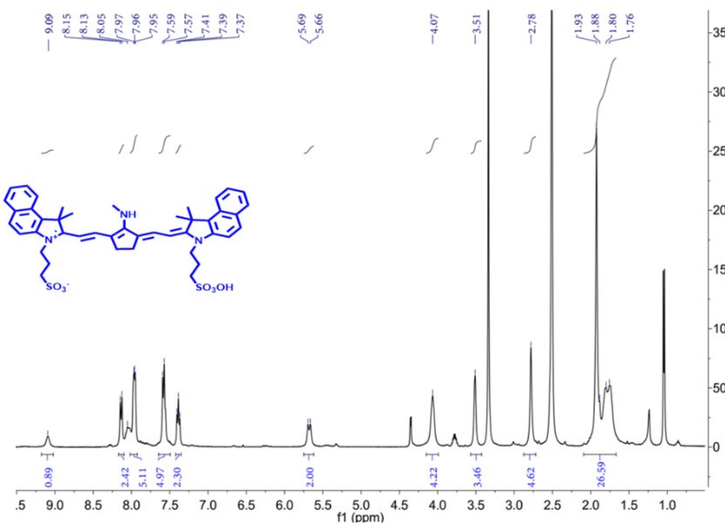

Fig. S4 ^{1}H NMR spectrum of **Cy-N**

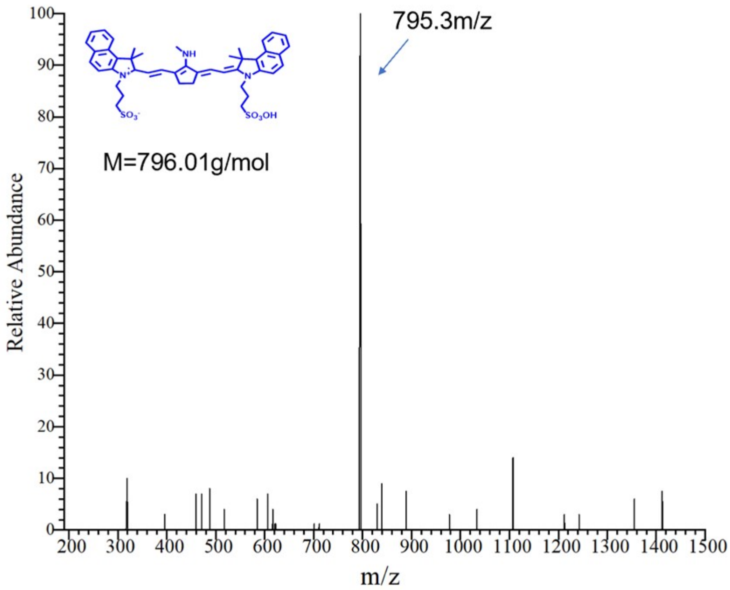

Fig. S5 ESI mass spectra spectrum of Cy-N

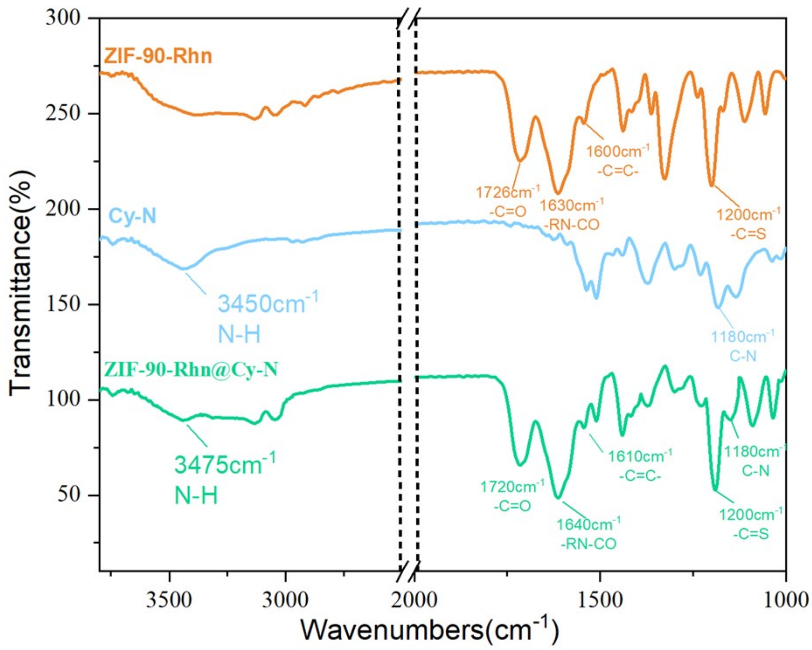

Fig. S6 The FT-IR spectra of **ZIF-90-Rhn**, **Cy-N**, **ZIF-90-Rhn@Cy-N**.

In Fig. S6: The FT-IR spectrum of **ZIF-90-Rhn@Cy-N** was investigated as shown in Figure 5 to further confirm the encapsulating of **ZIF-90-Rhn** for **Cy-N**. The bands at 1726, 1630, 1600, 1200 cm^{-1} belonged to the vibrational absorption peaks of carbonyl (-COOH, HN-CO), C=C and thione (-C=S) groups in **ZIF-90-Rhn** molecule. The weak peaks at 3450 cm^{-1} and 1180cm^{-1} could be attributed to the -N-H and -C-NH stretching vibration peak which stemmed from the **Cy-N** separately. However, the characteristic peaks of carbonyl (-COOH, HN-CO), C=C, and -N-H groups belonged to **ZIF-90-Rhn@Cy-N** changed and formed new peaks in 1720 cm^{-1}, 1640 cm^{-1}, and 1610 cm^{-1}, which showed that **Cy-N** had successful doped into **ZIF-90-Rhn**, and **ZIF-90-Rhn@Cy-N** had been generated.

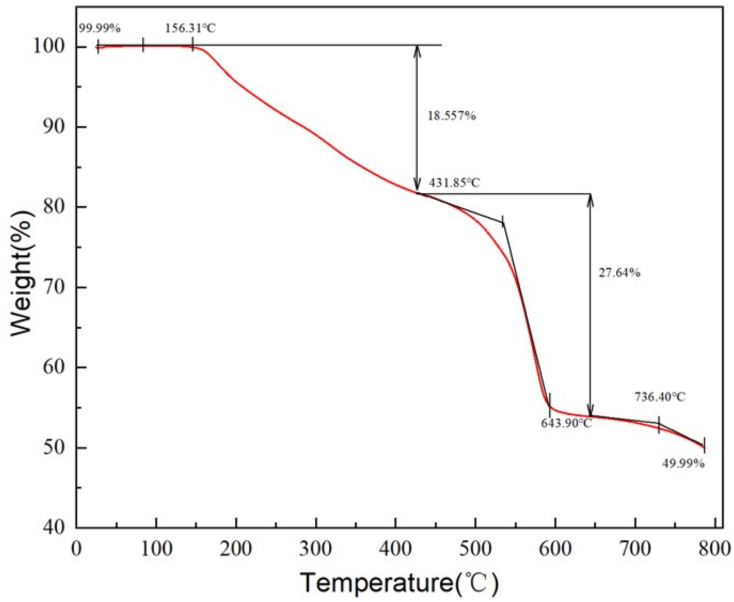

Fig. S7 Thermogravimetric analysis (TGA) of **ZIF-90-Rhn(a)** in an air atmosphere in the temperature range of 50-800 °C with a heating rate of 10 °C min^{-1}.

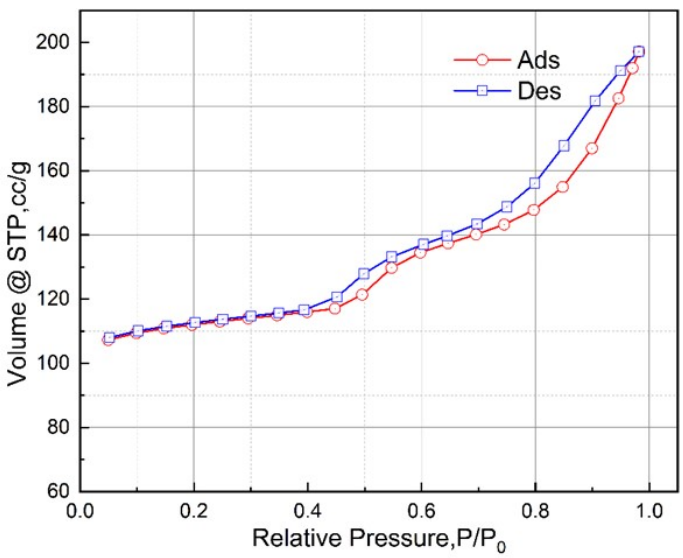

Fig. S8 N_2 adsorption (black curve) and desorption (red curve) isotherms of **ZIF-90-Rhn(a)** recorded at –195.8 °C.

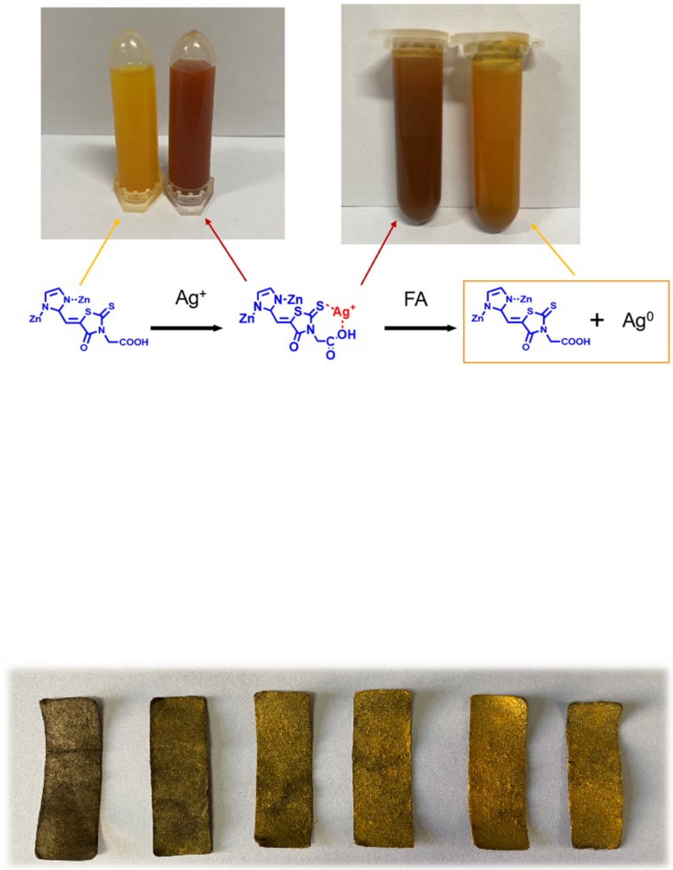

Fig. S9 The phenomenon of original experiment.

S1 Calculation of pH for Ag^+ to form the precipitation of AgOH

According to the K_{sp} calculation formula (1) of AgOH:

$$K_{sp} = c(Ag^+) \times c(OH^-) = 2.0 \times 10^{-8} \quad 25°C \qquad (1)$$

The concentration of Ag^+ used in this experiment was 100 μM. Thus, when OH^- concentration was 2.0×10^{-4} M, Ag^+ would start to form precipitation of AgOH. According to the pH calculation formula (2):

$$pH = 14 - \lg c(OH^-) \quad 25°C \qquad (2)$$

With 2.0×10^{-4} M of OH^-, the solution pH is 10.3.

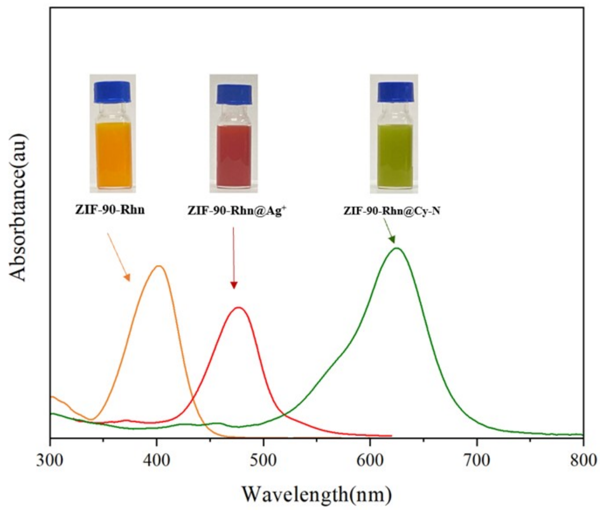

Fig. S10 UV-vis spectra of **ZIF-90-Rhn**, **ZIF-90-Rhn@Ag$^+$** and **ZIF-90-Rhn@Cy-N**

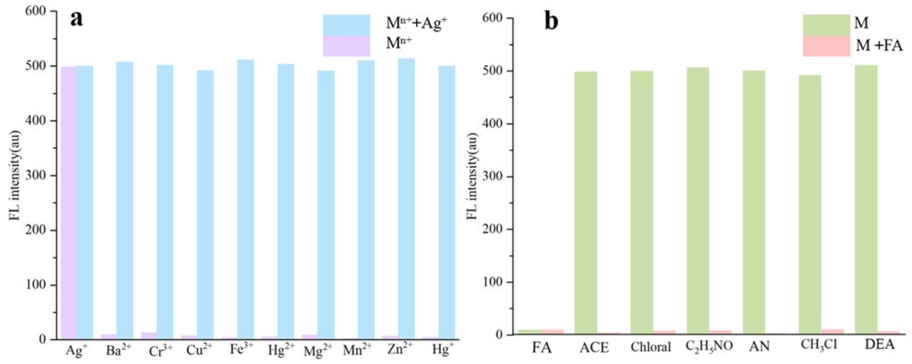

Fig. S11 Anti-interference ability of **ZIF-90-Rhn@Cy-N**, λ_{ex} = 678 nm, λ_{em} = 722 nm

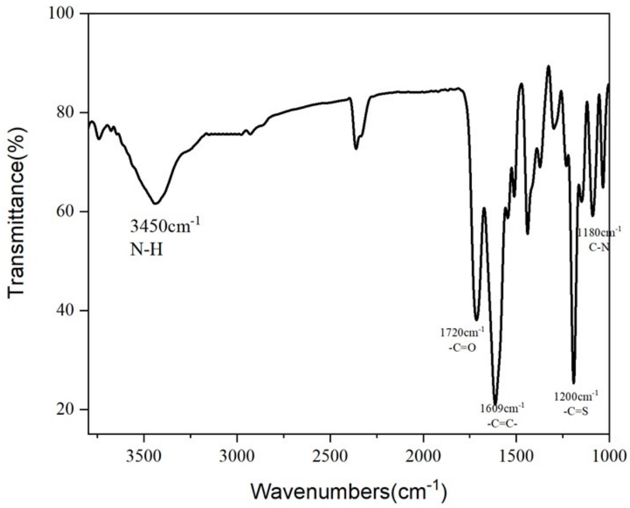

Fig. S12 The FT-IR spectra of analyte after identification of Ag^+ and FA

In Fig. S12: The compound after **ZIF-90-Rhn@Cy-N** continuously recognizes Ag^+ and formaldehyde was measured. The bands at 1180,1200, 1609, 1720 and 3450 cm^{-1} belong to the vibrational absorption peaks of the **ZIF-90-Rhn@Cy-N** molecule.

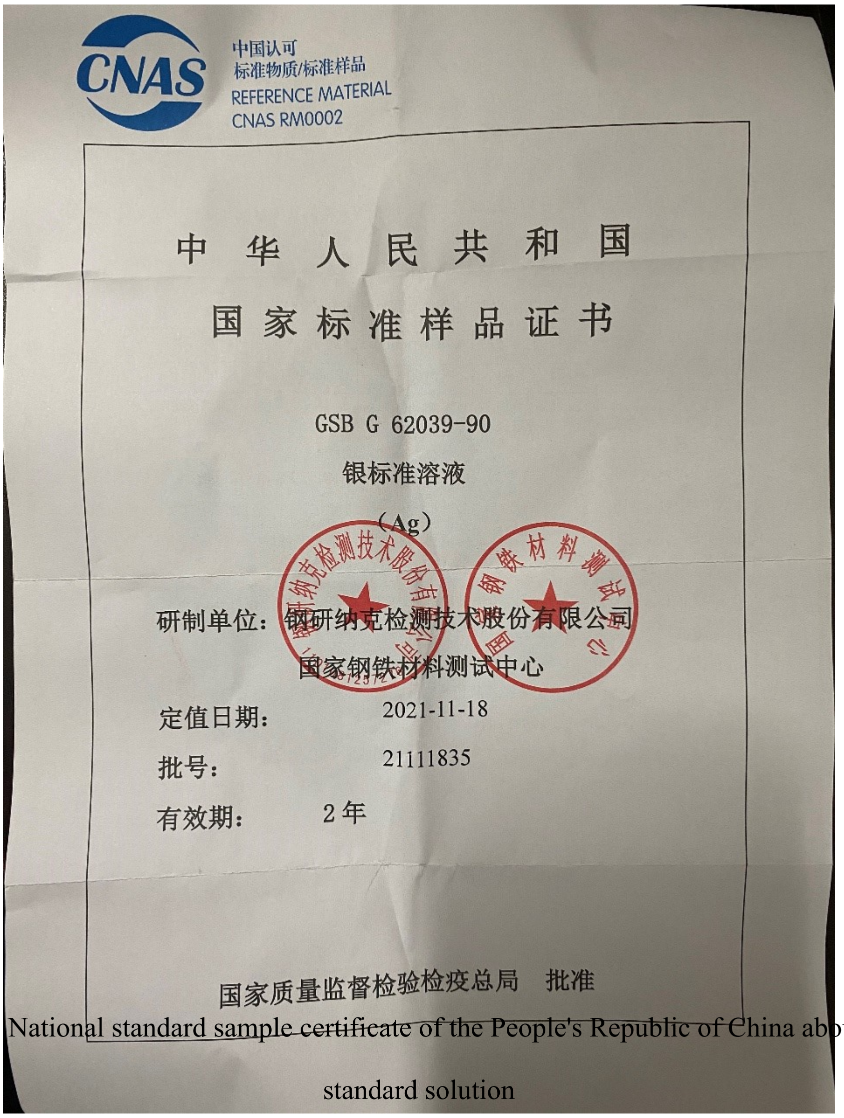

中国认可
标准物质/标准样品
REFERENCE MATERIAL
CNAS RM0002

中 华 人 民 共 和 国

国 家 标 准 样 品 证 书

GSB G 62039-90

银标准溶液

（Ag）

研制单位：钢研纳克检测技术股份有限公司

国家钢铁材料测试中心

定值日期： 2021-11-18

批号： 21111835

有效期： 2 年

国家质量监督检验检疫总局 批准

Fig. S13 National standard sample certificate of the People's Republic of China about silver standard solution

S2: Calculation of removal rate

The removal rates of Ag^+ and FA could be calculated in this way:

Removal rate = (initial conc. -final conc.) / initial conc. × 100%

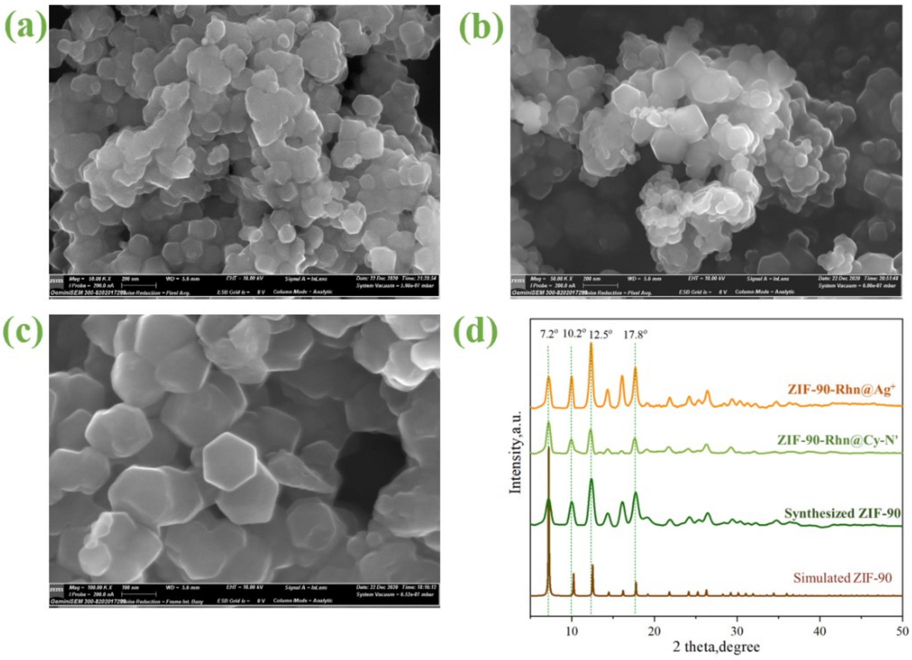

Fig. S14 (a) The SEM of **ZIF-90-Rhn@Ag$^+$**. (b) The SEM of **ZIF-90-Rhn@Cy-N'.** (c) The SEM of **ZIF-90.** (d) The PXRD of **ZIF-90-Rhn@Ag$^+$**, **ZIF-90-Rhn@Cy-N'**, **ZIF-90** and Simulated **ZIF-90.**

The **ZIF-90-Rhn@Cy-N’** product was employed to removal Ag^+ and FA and this process had been repeated for three recycles. It could be seen in Figure S14, **ZIF-90-Rhn@Cy-N’** was able to remove Ag^+ and FA as well, and after three recycles, the removal rate was up to respectively, which demonstrated that probe **ZIF-90-Rhn@Cy-N** could be reused for the removal of Ag^+ and FA.

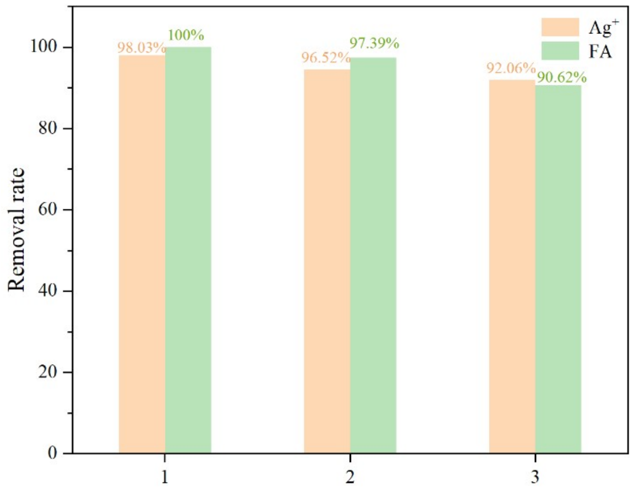

Fig. S15 The removal rate of **ZIF-90-Rhn@Cy-N’** product for the removal of Ag^+ and FA with three recycles.

Table S1. Comparation of ZIF-90-Rhn@Cy-N with reported Ag^+ sensors

Ref.	Sensor Material	Detection limit	response time
1	Sm^{3+}@MIL-121	0.09 μM	30 min
2	AuNPs	0.41 μM	3 min
3	3D MOF-MoS_2NB	0.25 nM	2 h
4	GR-5/GC DNAzyme	4.2 nM	30 min
5	Metal−Polydopamine	34 pM	10 min
6	Europium-Based Probe	9 nM	-
7	OPDA	60 nM	-
8	FA-CDs@Eu-MOFs-based	80 pM	-
9	Cys@Fe_3O_4Nps	0.1 nM	150 s
10	Si-CDs@DA	2.5 nM	
This work	ZIF-90-Rhn@Cy-N	0.56 μM	3 min

Table S2. Comparation of ZIF-90-Rhn@Ag^+/Cy-N with reported FA sensors

Ref.	Sensor Material	Detection limit	response time (s)
11	Al-MIL-53-NH_2	8.37 μM	60
12	Zr-UiO-66-NH_2	4.0 μM	120
13	Eu/Zr-UiO-66-NH_2	6.7 μM	-
14	Ag^+/Eu^{3+}-UiO-66	1.7 μM	360
15	ZIF-90-LW	2.3 μM	28
16	Na-FA	7.1×10^{-7} M	1800

17	FP1	0.01 mM	10800
18	FAP	0.5 μM	7200
19	RFAP	0.3 μM	7200
20	probe 1	900 nM	-
This work	ZIF-90-Rhn@Ag^+/Cy-N	2.16	300

Table S3 Comparation of ZIF-90-Rhn@Cy-N with reported Ag^+ adsorbent

Ref.	**Sensor Material**	**removal time**	**removal efficiency**
21	TiO_2-Based Photocatalysis	30 min	100%
22	MoS_2	-	99%
23	Mo_3S_{13}−Ppy	1h	99%
24	MoS_4-LDH	6 h	99.5%
25	poly(S_{40}-r-$DOBP_{60}$)	24 h	100%
This work	ZIF-90-Rhn@Cy-N	3 min	100%

Table S4 Comparation of ZIF-90-Rhn@Ag^+ /Cy-N with reported FA adsorbent

Ref.	**Sensor Material**	**removal time**	**removal efficiency**
	AlOOH	42 min	100%
	PPCT/KOH	4 h	93%
	UiO-66-NH_2	48 h	93%
	MnO_2/ AlOOH	40 min	52%
	BN layer	30 min	83%

This work	ZIF-90-Rhn@ Ag^{+}/Cy-N	3 min	97%

References

1 H. Ji-Na, Y. Bing, *Journal of Materials Chemistry A*, 2015, **3**, 4788.

2 B. Jie, X. Yunxia, S. Luyan, Z. Chenxue, L. Yuxi, L. Guiying Li, L. Xunyong, W. Xing, L. Yi, *New J. Chem*, 2020, **44**, 5438.

3 P. Rajaji, A. Arunjegan, S. Sivanesan, P. Panneerselvam, *ACS Appl. Mater. Interfaces*, 2021, **13**, 31710−31724.

4 R, Pavadai, P. Perumal, *ACS Omega*, 2020, **5**, 25188−25198.

5 R. Ayyanu, P. Perumal, M. Norhashimah, ACS Appl. Mater. Interfaces 2018, *10*, 20550−20558.

6 I. Manon, D. Sergey A., M. Nathan D., S. Olivier, *Inorg. Chem*, 2021, **60**, 10791−10798.

7 Y. Xuan, W. Erkang, *Anal. Chem*, 2011, **83**, 5005–5011.

8 Z. Yuanhua, Z. Kai Zhou, Q. Yan, X. Lan, X. Zhining, Z. Kailian, F. Qifeng, *Sensors & Actuators: B*, Chemical 339 **(2021)** 129922.

9 A. Arunjegan, P. Rajaji, P. Panneerselvam, *ACS Omega*, 2021, **6**, 30580−30597.

10 J. Yuliang, W. Zhaoyin, D. Zhihui, *ACS Appl. Mater. Interfaces*, 2016, **8**, 3644−3650.

11 22 S. Nandi, E. Sharma, V. Trivedi and S. Biswas, *Inorg. Chem*., 2018, **57**, 15149–15157.

12 K. Vellingiri, A. Deep, K.-H. Kim, D. W. Boukhvalov, P. Kumar, Q. Yao, *Sens. Actuators, B*, 2017, **241**, 938–948.

13 C. Li, J. Huang, H. Zhu, L. Liu, Y. Feng, G. Hu, X. Yu, *Sens. Actuators, B*, 2017, **253**, 275–282.

14 J. N. Hao, B. Yan, *Nanoscale*, 2016, **8**, 12047–12053.

15 M. W. Li, A. Shen, Y. Q. Liang, H. Zhen, X. H. Hao, X. L. Liu, X. C. Sun, Y. X. Yang, *Anal. Methods*, 2020, **12**, 3748–3755.

16 A. Roth, H. Li, C. Anorma, J. Chan, *J. Am. Chem. Soc.*, 2015, **137**, 10890–10893.

17 Z. Li, Y. Xu, H. Zhu, Y. Qian, *Chem. Sci.*, 2017, **8**, 5616–5621.

18 T. F. Brewer, G. Burgos-Barragan, N. Wit, K. J. Patel, C. J. Chang, *Chem. Sci.*, 2017, **8**, 4073–4081.

19 C. Liu, C. Shi, H. Li, W. Du, Z. Li, L. Wei M. Yu, Sens. *Actuators, B*, 2015, **219**, 185–191.

20 W. Zhou, H. Dong, H. Yan, C. Shi, M. Yu, L. Wei Z. Li, *Sens. Actuators, B*, 2015, **209**, 664–669.

21 H. Min, E rwintso, Abhayak, Datye, *Environ. Sci. Technol*. 1996, **30**, 3084-3088.

22 W. Zhongying, S. Alison, U. Jeffrey J., M. Baoxia, *Environ. Sci. Technol*, 2018, **52**, 9741−9748.

23 Y. Mengwei, Y. Huiqin, X. Linxia, L. Xiaowen, W. Hui, I. Saiful M, S. Keren, Y. Zihuan, S. Genban, L. Huifeng, M. Shulan, K. Mercouri G., *J. Am. Chem. Soc*. 2020, **142**, 1574−1583.

24 M. Lijiao Ma, W. Qing, I. Saiful M., L. Yingchun, M. Shulan, K. Mercouri G., *J. Am. Chem. Soc*. 2016, **138**, 2858−2866.

25 K. Li-An, H. Yun-Syuan, L. Yuya A., *ACS Appl. Polym. Mater*. 2021, **3**, 3363−3372.

26 X. Zhihua, Y. Jiaguo, L. Jingxiang, J. Mietek, *ACS Appl. Mater. Interfaces*, 2014, **6**, 2111−2117.

27 S. Shasha, S. Aixin, F. Lei, W. Guangcheng, D. Shuli Dong, H. Jingcheng, *ACS Appl. Mater. Interfaces*, 2014, **6**, 18319−18328.

28 V. Kowsalya, D. Ya-Xin, K. Ki-Hyun, J. Jheng-Jie Jiang, K. Taejin, S. Jin, A. Wha-Seung, K. Deepak, B. Danil W., *ACS Appl. Mater. Interfaces*, 2019, **11**, 1426−1439.

29 L. Zhiyuan, N. Jingpeng, L. Weimin, C. Bing, S. Kun Song, D. Fan, X. Dong, *Inorg. Chem*. 2020, **59**, 7335−7343.

30 Y. Jiawei, Z. Xiaofeng, C. Bei, Y. Jiaguo, J. Chuanjia, *Environ. Sci. Technol. Lett.*, 2017, **4**, 20−25.